Stable Iron Isotope Fractionation Between Aqueous Fe(II) and Hydrous Ferric Oxide

4 AUTHORS, INCLUDING:

Lingling Wu
University of Waterloo
24 PUBLICATIONS   **509** CITATIONS

Stable Iron Isotope Fractionation Between Aqueous Fe(II) and Hydrous Ferric Oxide

Lingling Wu,[†,‡,*] Brian L. Beard,[†,‡] Eric E. Roden,[†,‡] and Clark M. Johnson[†,‡]

[†]Department of Geoscience, University of Wisconsin-Madison 1215 West Dayton Street, Madison, Wisconsin 53706, United States
[‡]NASA Astrobiology Institute, University of Wisconsin-Madison Madison, Wisconsin 53706, United States

Ⓢ *Supporting Information*

ABSTRACT: Despite the ubiquity of poorly crystalline ferric hydrous oxides (HFO, or ferrihydrite) in natural environments, stable Fe isotopic fractionation between HFO and other Fe phases remains unclear. In particular, it has been difficult to determine equilibrium Fe isotope fractionation between aqueous Fe(II) and HFO due to fast transformation of the latter to more stable minerals. Here we used HFO stabilized by the presence of dissolved silica (2.14 mM), or a Si—HFO coprecipitate, to determine an equilibrium Fe(II)—HFO fractionation factor using a three-isotope method. Iron isotope exchange between Fe(II) and HFO was rapid and near complete with the Si—HFO coprecipitate, and rapid but incomplete for HFO in the presence of dissolved silica, the latter case likely reflecting blockage of oxide surface sites by sorbed silica. Equilibrium Fe(II)—HFO $^{56}Fe/^{54}Fe$ fractionation factors of -3.17 ± 0.08 (2σ)‰ and -2.58 ± 0.14 (2σ)‰ were obtained for HFO plus silica and the Si—HFO coprecipitate, respectively. Structural similarity between ferrihydrite and hematite, as suggested by spectroscopic studies, combined with the minor isotopic effect of dissolved silica, imply that the true equilibrium Fe(II)—HFO $^{56}Fe/^{54}Fe$ fractionation factor in the absence of silica may be ~ -3.2‰. These results provide a critical interpretive context for inferring the stable isotope effects of Fe redox cycling in nature.

■ INTRODUCTION

Iron oxides and hydroxides are important components of the Fe cycle in sedimentary environments, reflecting the end product of Fe(II) oxidation, as well as substrates for microbial dissimilatory iron reduction. Hydrous ferric oxide (HFO, or ferrihydrite) is a common precursor to goethite and hematite, and is ubiquitous in soils and sediments.[1] HFO plays a significant role in scavenging contaminants from environments by adsorption and coprecipitation due to its extremely high surface area and reactivity.[2] Stable Fe isotope fractionation studies of iron oxy-(hydro)xide have provided important insights into Fe redox transformations in both ancient and modern environments,[3] as well as their reactivity.[4] Although stable Fe isotope fractionations between aqueous ferrous iron and iron oxy-(hydro)xides have been studied extensively (Table 1), the equilibrium fractionation factor between aqueous Fe(II) and HFO remains unknown, and thus presents a significant hindrance to interpreting Fe redox cycling in nature. Studies of Fe(II)—HFO interactions are difficult because HFO rapidly transforms into more crystalline, thermodynamically stable forms, such as lepidocrocite and goethite in the presence of ferrous iron,[1,5] or reacts to form mixed Fe(II)—Fe(III) minerals such as magnetite.[6]

In this study we used either dissolved silica (2.14 mM) in solution or a Si—HFO coprecipitate (referred to as Si—HFO) to stabilize HFO, and hence determine equilibrium Fe isotope fractionation between Fe(II) and HFO using a three-isotope method. The three-isotope method was employed to rigorously document the isotopic fractionation factor that would be achieved at complete isotope exchange, and the results thus likely represent the equilibrium isotope fractionation factor.[7,8] Dissolved Si is a common species in natural waters and was also important in Precambrian marine systems prior to development

of silica-secreting organisms.[9] Silica species have long been recognized as an effective means to stabilize HFO and inhibit its transformation to more stable minerals.[10–12] Adsorption of Si reduces the direct adsorption of aqueous Fe(II), thereby potentially hindering the extent of atom/electron exchange between aqueous Fe(II) and Fe(III) within the mineral structure.[10] In addition, upon dissolution of HFO following electron exchange with aqueous Fe(II), Si prevents recrystallization into a more stable Fe(III) or mixed Fe(II)—Fe(III) mineral by restricting crystal growth via sorption to growth sites.[13,14] We used the structural similarity between HFO and hematite, as revealed by earlier spectroscopic studies (e.g., refs 15–17), and the minor isotopic effect of dissolved silica on Fe(II)$_{aq}$—HFO interactions, to infer the true equilibrium fractionation factor between Fe(II)$_{aq}$ and HFO in the absence of silica.

■ MATERIALS AND METHODS

Materials. A stock solution of ferrous Fe with a "normal" isotopic composition was prepared by dissolving $FeCl_2 \cdot 4H_2O$ in 0.5 M HCl in an anaerobic chamber (Coy Products, Grass Lake, MI). A ^{57}Fe-enriched ferrous stock solution was prepared by dissolving pure ^{57}Fe metal (Chemgas) in HCl and mixing it with isotopically "normal" ferrous solution in an anaerobic chamber. Hydrous ferric oxide was synthesized by rapid hydrolysis of either isotopically "normal" or ^{57}Fe-enriched $FeCl_3$ solution with NaOH until pH reached 7, followed by washing the solid gel 4 times with

Table 1. Experimentally Determined Fe Isotope Fractionation Factors at 20 °C between $Fe(II)_{aq}$ and $Fe(III)_{aq}$ or Fe(III) Oxy-(hydro)xides[a]

	$\Delta^{56}Fe$
$Fe(II)_{aq}$ - $Fe(III)_{aq}$	-3.01 [21,22]
$Fe(II)_{aq}$ - hematite	-3.16 [22,41]
$Fe(II)_{aq}$ - goethite	-1.05 [7]
$Fe(II)_{aq}$ - natural Fe(III) oxide-rich sediments	~-2 [42]
$Fe(II)_{aq}$ - Si-HFO	-2.58
$Fe(II)_{aq}$ - HFO[b]	-3.17
$Fe(II)_{aq}$ - HFO[c]	~-3.2

[a] Note all aqueous species are hexaquo complexes. [b] in presence of dissolved silica. [c] estimated for pure $Fe(II)_{aq}$-HFO system based on minor inferred effect from dissolved silica (see text).

H_2O. XRD showed that HFO remains X-ray amorphous over the course of the experiments. TEM work showed that HFO had an average diameter of ~3 nm. A Si−HFO coprecipitate was synthesized by rapid hydrolysis of either isotopically "normal" or ^{57}Fe-enriched $FeCl_3$ solution in the presence of equal molarity of dissolved silica with NaOH, until pH reached 7; the solid gel was then also washed 4 times with H_2O. XRD showed that both ^{57}Fe-enriched and isotopically "normal" Si−HFO remained X-ray amorphous over the course of the experiments. TEM work showed that Si−HFO has an average diameter of ~3 nm.

Experimental Design. Four sets of experiments were conducted: (1) ^{57}Fe-spiked Fe(II) + "normal" HFO; 2) "Normal" Fe(II) + ^{57}Fe-spiked HFO; 3) ^{57}Fe-Spiked Fe(II) + "normal" Si−HFO; 4) "Normal" Fe(II) + ^{57}Fe-spiked Si−HFO. Duplicate reactors were set up for each set of experiment. Experiments 1 and 2 were carried out in separate 10 mL serum glass bottles with 10 mL anoxic (N_2-bubbled) Pipes buffer (10 mM) that contained 2.14 mM silica (added as $Na_2SiO_3 \cdot 9H_2O$) and 2 mM HFO. Experiments 3 and 4 were carried out in a similar fashion, except the Pipes buffer did not contain dissolved silica. The experiments were initiated by addition of $FeCl_2$ from an anaerobic stock solution. The pH of the solutions was adjusted to be ~7. Experiments 1 and 2 were conducted for 28 days and experiments 3 and 4 were conducted for 30 days. All sampling was carried out in an anaerobic chamber. The experiments were conducted at room temperature (20 °C); where temperature was stable to ±1 °C over the course of the experiments.

Fe Phase Separation and Wet Chemical Analysis. Bottles that contained 10 mL aliquots of the reaction slurries were centrifuged (3600 rpm, 10 min) to remove the aqueous fraction $(Fe(II)_{aq})$ after certain periods of time. For experiments 1 and 2, the remaining solids were extracted for 10 min using 5 mM HCl (reagent grade), which removed the majority of sorbed Fe(II) without dissolving any underlying Fe(III), as was confirmed by Fe(II) and total Fe measurements. Fe(II) and total Fe concentrations were measured using *Ferrozine* and hydroxylamine hydrochloride as a reductant for Fe(III),[18] and Fe(III) was determined by difference. A second extraction using 10 mM HCl for 5 min dissolved a small amount of HFO based on trial tests. For experiments 3 and 4, the first extraction was done using 5 mM HCl for 5 min, and no second extraction was performed, except for the initial time point, where the solid was extracted using 10 mM HCl for 2 min. The remaining solids were dissolved using 0.5 M HCl for overnight for all experiments. Silica concentrations for different fractions were analyzed using a colorimetric method.[19]

Fe Isotope Analysis. Samples of $Fe(II)_{aq}$, acid extractions, and bulk HFO and Si−HFO were purified using anion-exchange chromatography before analyzed by a multicollector, inductively coupled plasma mass spectrometer (MC-ICP-MS) following established protocols.[7] A fast washout spray chamber, and a decreased potential difference between extraction and skimmer cones, were employed to avoid memory effects. All isotopic compositions are reported as $\delta^{56}Fe$ and $\delta^{57/56}Fe$ values, which reflect the $^{56}Fe/^{54}Fe$ and $^{57}Fe/^{56}Fe$ ratios, respectively, relative to the baseline of terrestrial igneous rocks.[7,20] External precision for $\delta^{56}Fe$ and $\delta^{57/56}Fe$ values are both 0.05‰ (1σ), as determined by replicate analysis of 84 samples, including 29 samples separately processed through anion-exchange chromatography, out of 277 samples reported in Tables S1 to S3 in the Supporting Information (SI).

RESULTS AND DISCUSSION

Kinetics of Isotope Exchange Governed by Competitive Sorption of Fe and Silica. XRD and TEM indicated that the solids remained amorphous throughout all of the isotope exchange experiments (SI Figures S1 and S2). There was no change of particle size as observed by TEM (SI Figure S2). Aqueous Fe(II) $(Fe(II)_{aq})$ and bulk HFO dominated Fe mass balance in the experiments; two weak HCl extractions of the solid provided subsampling of a smaller portion (ca. 10−20%) of total Fe (SI Figures S3 and S4). The molar proportion of each component remained unchanged during experiments with HFO in silica-containing solution (Experiments 1 and 2, which are referred to hereafter as the HFO+Si experiments). In contrast, the molar proportion of $Fe(II)_{aq}$ decreased with time in experiments with the Si−HFO coprecipitate (Experiments 3 and 4, which are referred to hereafter as the Si−HFO experiments). The decrease in $Fe(II)_{aq}$ was accompanied by an increase of weak HCl-extractable Fe(II), reflecting net mass transfer of Fe(II) from aqueous to solid phase with time. This conclusion was verified by the increasing amount of Fe(II) recovered in the bulk Si−HFO dissolution (SI Table S4).

The fraction of isotope exchange can be described by $F = (\delta - \delta_i)/(\delta_e - \delta_i)$, where δ is the isotopic composition at any time, δ_i is the isotopic composition of the starting material, and δ_e is the equilibrium isotope composition calculated from the mass balance of each reactor. The mass balance of the system was constrained within a 3% error (1 standard deviation divided by the mean) for HFO+Si experiments and within a 4% error for Si−HFO experiments. Calculation of F using either aqueous Fe(II) or HFO agreed within 9% (difference between the values calculated from $Fe(II)_{aq}$ or HFO) for HFO+Si experiments, and within 3% for Si−HFO experiments (see SI Table S5). $\delta^{57/56}Fe$ values were used to calculate F because a ^{57}Fe-enriched tracer was used, minimizing the effects of mass-dependent fractionation in estimating δ_e. For all experiments, the initial time point (sampled 30 min after mixing) showed a significant change in isotopic composition relative to the starting materials (Figure 1; see also SI Figures S3 and S4), reflecting rapid initial isotopic exchange.

The relation between fraction of exchange (F) and time cannot be described by a simple second order reaction, as shown for isotopic exchange between aqueous Fe(II) and aqueous Fe(III).[21,22] Instead, the temporal trends in isotopic exchange indicate that competitive sorption of Fe and silica to surface sites on HFO controlled the kinetics of the isotopic exchange.

In HFO+Si experiments, isotopic exchange was rapid initially and then leveled off at ~50% from 10 to 28 days (Figure 1). The sluggishness of isotopic exchange in these experiments may be explained by blockage of reactive surface sites by silica transferred from aqueous to solid phase. We infer that adsorbed silica was strongly bound to surface Fe in HFO, possibly also to Fe
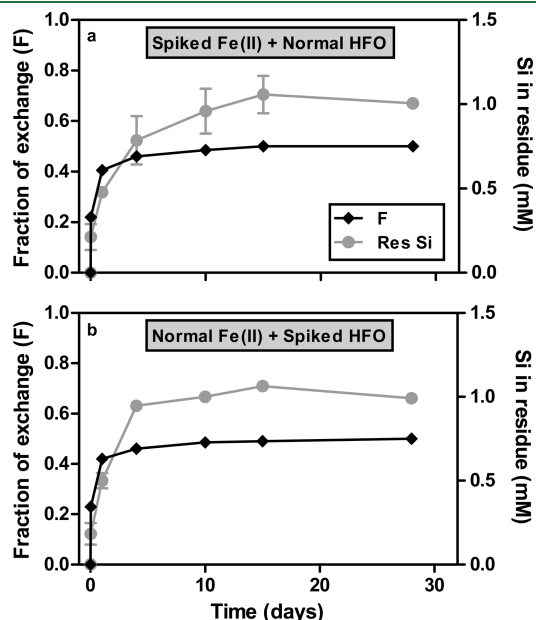

Figure 1. Temporal variations in the fraction of isotopic exchange (F) and silica concentrations in the residue for HFO+Si experiments. Error bars indicate one standard error of the mean from duplicate reactors. The plot shows that isotopic exchange was rapid initially and then leveled off at ~50% exchange, which is interpreted to reflect blockage of reactive surface sites by increased incorporation of silica in the HFO residue. Data from SI Tables S5 and S6.

deeper in the structure, hindering further isotopic exchange after 10 days. Surface complexation modeling has shown that silica species bind directly to iron oxide/hydroxide surfaces through inner-sphere complexes,[23] which should inhibit atom exchange between Fe(II) and Fe(III) in HFO. Mass transfer of silica from aqueous to solid, and its subsequent strong binding with HFO, can be observed in the increase in silica in the solid phase that could not be removed by weak HCl leaching (Figure 1). The relatively sluggish Fe isotope exchange observed in this study is in contrast with ~80% isotopic "exchange" observed between Fe(II)$_{aq}$ and ferrihydrite in a previous study using ^{55}Fe tracer,[5] although it is important to note that phase transformations occurred in the ^{55}Fe tracer experiments and therefore these did not reflect true isotopic exchange reactions.

Iron isotope exchange was rapid in the Si—HFO experiments and went to near-completion after 9 days (Figure 2a,b). Upon mixing, silica moved from solid to aqueous phase (Figure 2c,d). The liberation of Si into solution presumably freed reactive surface sites, thus promoting isotopic exchange between Fe(II) and the Si—HFO relative to the HFO+Si experiments. The transport of silica to solution could also be detected by a decline in the amount of solid-phase silica recovered by a brief (5 min) extraction with 5 mM HCl (Extract 1 in SI Table S6). A similar effect of net loss of Si from Si—HFO structure was observed by Jones et al.[10] Silica mass transfer was accompanied by transfer of Fe from the aqueous to the solid-phase (Figure 2c,d; SI Table S4). Although the Fe:Si ratios of the Si—HFO solid remained constant throughout the experiment, the amount of Fe(II) increased with time (SI Table S4), reflecting the transfer of electrons leading to in situ reduction of Fe(III). Coupled atom and electron exchange has been shown to be the mechanism for Fe isotope fractionations during dissimilatory Fe(III) oxide reduction,[24,25] as well as abiotic aqueous Fe(II)—hematite surface interactions.[26] Therefore, we infer that this transfer of electrons facilitated atom exchange between Fe(II) and Si—HFO,
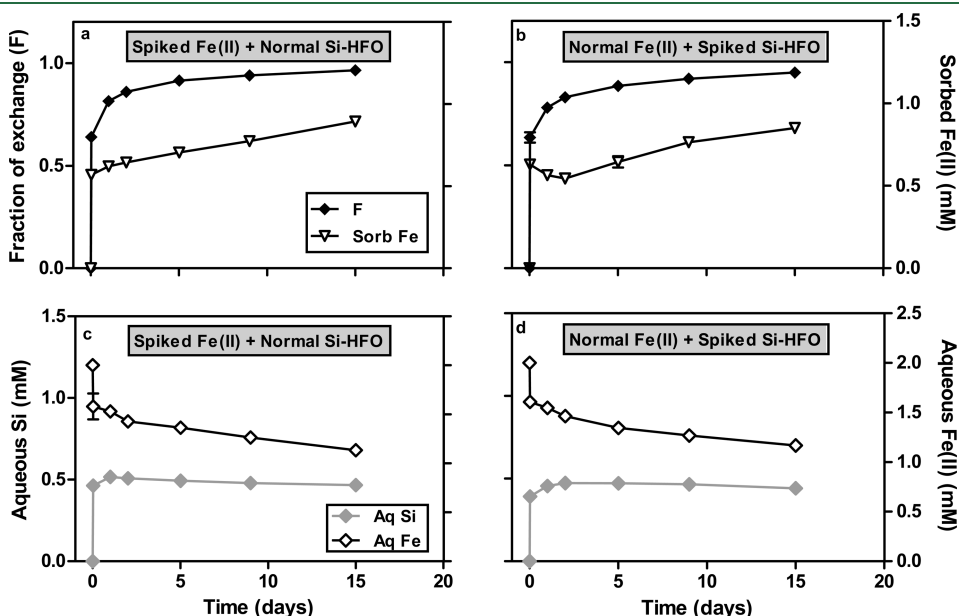
Figure 2. Temporal variations in the fraction of isotopic exchange (F) and sorbed Fe(II) concentrations (a and b), as well as aqueous Fe and silica concentrations (c and d), for Si—HFO experiments. Error bars indicate one standard error of the mean from duplicate reactors. The last two time points were not plotted because the batch was prepared separately and followed a different trend. The plot shows that isotopic exchange was rapid initially and went to near completion, which is interpreted to result from Fe replacement of silica in the Si—HFO. Data from SI Tables S4—S6.
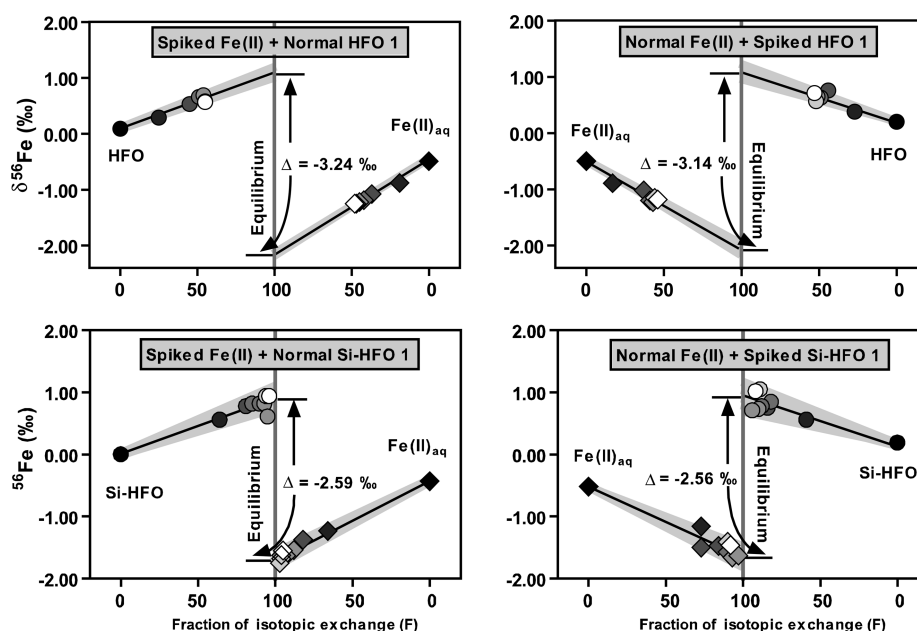
Figure 3. Plot of isotopic composition versus fraction of isotopic exchange (F). Isotopic compositions at equilibrium were obtained by extrapolation to 100% isotopic exchange. Symbols are shaded where the darkest symbols represent starting materials and the lightest symbols represent final time points. The data are from one set of the duplicate reactors, and are representative of both reactors.

Table 2. Extrapolated Fe Isotope Composition of Aqueous Fe(II) and HFO or Si−HFO at Equilibrium[a]

experiment	$Fe(II)_{aq}$ $\delta^{56}Fe$	$(Si-)HFO$ $\delta^{56}Fe$	$\Delta^{56}Fe_{Fe(II)aq-(Si-)HFO}$
spiked Fe(II) + normal HFO 1	−2.15	1.09	−3.24 ± 0.14
spiked Fe(II) + normal HFO 2	−2.13	1.05	−3.18 ± 0.14
normal Fe(II) + spiked HFO 1	−2.05	1.09	−3.14 ± 0.23
normal Fe(II) + spiked HFO 2	−2.08	0.97	−3.05 ± 0.19
spiked Fe(II) + normal Si−HFO 1	−1.69	0.90	−2.59 ± 0.25
spiked Fe(II) + normal Si−HFO 2	−1.68	0.92	−2.60 ± 0.28
normal Fe(II) + spiked Si−HFO 1	−1.63	0.92	−2.56 ± 0.33
normal Fe(II) + spiked Si−HFO 2	−1.64	0.91	−2.55 ± 0.28
weighted average for all HFO+Si experiments			−3.17 ± 0.08 (2σ)
weighted average for all Si−HFO experiments			−2.58 ± 0.14 (2σ)

[a] Extrapolated Fe isotope compositions are based on using a straight line best fit to all the time points for each component to the equilibrium line via forcing the best-fit line to go through the initial $Fe(II)_{aq}$ or solid ferric component (see Figure 3). Errors of fractionation factor for each experiment were calculated by propagating errors for two extrapolated equilibrium values. Errors for weighted average fractionation factor were calculated by Isoplot based on four experiments.

as seen by the near complete isotopic exchange in the Si−HFO experiments. Comparison of these results with those of Poulson et al.,[27] who noted only limited isotopic exchange between $Fe(III)_{aq}$ and HFO—a system where there was no redox-driven electron exchange—illustrates the importance of electron transfer in promoting atom exchange.

Equilibrium Fractionation Between Fe(II) and HFO. Extrapolation of the mass-dependent Fe isotope fractionations to complete exchange produces a weighted-average, equilibrium $^{56}Fe/^{54}Fe$ fractionation of $-3.17 \pm 0.08(2\sigma)$‰ between $Fe(II)_{aq}$ and HFO in the presence of silica, and $-2.58 \pm 0.14(2\sigma)$‰ between $Fe(II)_{aq}$ and Si−HFO (Figure 3, Table 2). These two fractionation factors are very similar to the equilibrium fractionation

factors determined previously for $Fe(II)_{aq}$ and $Fe(III)_{aq}$, and $Fe(II)_{aq}$ and hematite (Table 1). The measured $^{56}Fe/^{54}Fe$ fractionation factor between $Fe(II)_{aq}$ and easily extractable (5 min leaching with 5 mM HCl), presumably surface-associated (i.e., sorbed) Fe(II) changed from −0.50‰ upon mixing to −0.75‰ after 28 days for HFO+Si experiments and from −0.75‰ upon mixing to −0.86‰ after 30 days for Si−HFO experiments (SI Table S3). These results suggest that, at equilibrium, the fractionation between $Fe(II)_{aq}$ and sorbed Fe(II) was ~−0.8‰. This fractionation factor lies between those determined previously for aqueous and sorbed Fe(II) during Fe(II)−goethite interactions $(-1.24 \pm 0.14‰)^{[7]}$ and during Fe(II)−hematite interactions $(-0.49 \pm 0.09‰).^{[25]}$

D

dx.doi.org/10.1021/es103171x |*Environ. Sci. Technol.* XXXX, XXX, 000–000

The possibility exists that formation of an Fe(II)−silica phase, perhaps catalyzed by HFO surfaces, could have influenced the measured equilibrium fractionation factor between Fe(II)$_{aq}$ and HFO. However, the results of HFO-free control experiments suggest that the impact of this phenomenon is likely to have been minor. The control experiments showed that ∼20% of total Fe(II) was sequestered in the solid phase in the absence of HFO, and that ∼8% of added Fe(II) was oxidized (SI Table S7). This partial oxidation of Fe(II) has also been observed in previous control experiments for Fe(II)−hematite interactions,[26] although the oxidant remains unknown for both cases, where complete recovery of added Fe(II) was achieved when hematite or HFO was present. Assuming a fractionation factor of −3.2‰ (see below) for Fe(II)$_{aq}$−Fe(III)−Si, mass balance calculations show that the isotope composition for Fe(II) in the precipitate (Fe(II)$_s$) was −0.4‰ (starting Fe(II)$_{aq}$ = −0.5‰), which produced a $^{56}Fe/^{54}Fe$ fractionation factor of −0.6‰ between Fe(II)$_{aq}$ and Fe(II)$_s$. This suggests that the isotopic composition of an Fe(II) silicate precipitate is similar to that of a sorbed component. Therefore, it is unlikely that silica affected the measured equilibrium Fe(II)$_{aq}$−HFO fractionation in a manner that is distinct from that of Fe(II) sorption. Nevertheless, it is possible that the presence of silica influenced Fe isotope fractionation in a different manner, perhaps through distortion of the structure of HFO relative to pure HFO without silica, as discussed below.

Equilibrium mass-dependent isotope fractionation is driven primarily by changes in molecular and crystalline vibration frequencies and reflects fundamental differences in bonding environments.[28,29] For example, the equilibrium Fe isotope fractionation factor between Fe(II)$_{aq}$ and goethite differs significantly from that of hematite (Table 1), reflecting important differences in the bonding environment of Fe in goethite as compared with hematite as revealed by spectroscopic[17,30−33] and theoretical[34,35] approaches. With respect to ferrihydrite, spectroscopic studies have revealed the presence of short Fe−Fe pairings and the existence of face-sharing Fe octahedra, pointing to the structural similarity between ferrihydrite and hematite in terms of Fe bonding (e.g., ref 15−17). Because bonding environment ultimately determines equilibrium stable isotope fractionation,[28] this structural similarity suggests that the true equilibrium fractionation factor between Fe(II) and HFO without silica may be close to that between Fe(II) and hematite. It is possible that silica distorted the bonding of surface iron atoms in HFO, leading to alteration in the equilibrium Fe isotope fractionation between Fe(II)$_{aq}$ and HFO. Such an effect of silica has been documented for the interaction of Fe(II)$_{aq}$ with reactive Fe(III) sites on the surface of hematite at elevated pH.[26] However, because only about 20% of Fe atoms are on the surface (calculated by assuming standard surface area of 600 m^2/g and site density of 2 sites/nm$^{2\ 36}$) and thus likely to be affected by Si distortion, we infer that the equilibrium fractionation factor between Fe(II) and bulk HFO, which was determined rigorously by the three-isotope method, should be affected minimally by dissolved silica. Collectively, these results imply that the equilibrium $^{56}Fe/^{54}Fe$ fractionation factor between Fe(II) and pure HFO in the absence of silica may be close to −3.2.

Implications for Interpretation of Fe Redox Cycles Based on Fe Isotopes. Changes in the redox state of Fe have been shown to produce a significant range in $\delta^{56}Fe$ values, from −5 to +1‰ in natural fluids and minerals;[37,38] diagenetically produced aqueous Fe(II) defines the lowest $\delta^{56}Fe$ values yet measured,

and Fe(III) oxide minerals generally define the highest $\delta^{56}Fe$ values measured. Although nonredox speciation changes, such as chlorinity, may influence Fe isotope fractionations, the effect is small in most natural aqueous systems (∼0.3‰/M Cl$^{-\ 39}$). The results of this study show that the Fe(II)$_{aq}$−HFO isotope fractionation factor is sufficiently large to explain the range in $\delta^{56}Fe$ values that have been inferred to reflect Fe redox cycling in natural systems. Moreover, the fact that under equilibrium conditions, fractionation between Fe(II)$_{aq}$ and HFO is very similar to that between Fe(II)$_{aq}$ and Fe(III)$_{aq}$ (Table 1) indicates that the Fe(III)$_{aq}$−HFO fractionation factor is near zero, which was previously inferred in experimental studies of biological Fe(II) oxidation.[40] Because Fe isotope exchange is sluggish between Fe(III)$_{aq}$ and HFO,[27] the current study demonstrates the importance of redox cycling (coupled electron and atom exchange), either biologically or abiologically, in producing significant Fe isotope variations observed in natural systems.

■ ASSOCIATED CONTENT

ⓢ Supporting Information. Eight figures showing XRD, TEM images, Fe concentrations, Fe isotope compositions, and $^{54}Fe/^{56}Fe$ vs $^{57}Fe/^{56}Fe$ for all the experiments and seven tables containing Fe, Si concentrations, Fe isotope measurements, including starting materials and control experiments and fraction of exchange for all the experiments. This material is available free of charge via the Internet at http://pubs.acs.org.

■ AUTHOR INFORMATION

Corresponding Author
*Phone: +1-608-890-0929; e-mail: lwu@geology.wisc.edu.

■ ACKNOWLEDGMENT

■ REFERENCES

(1) Cornell, R. M.; Schwertmann, U. The iron oxides: Structure, Properties, Reactions. In *Occurrences, and Uses Weinheim*: Wiley-VCH: New York, 2003; p 644.

(2) Michel, F. M.; Ehm, L.; Antao, S. M.; Lee, P. L.; Chupas, P. J.; Liu, G.; Strongin, D. R.; Schoonen, M. A. A.; Phillips, B. L.; Parise, J. B. The structure of ferrihydrite, a nanocrystalline material. *Science* **2007**, *316* (5832), 1726–1729.

(3) Johnson, C. M.; Beard, B. L.; Roden, E. E. The iron isotope fingerprints of redox and biogeochemical cycling in modern and ancient Earth. *Annu. Rev. Earth Planet. Sci.* **2008**, *36*, 457–493.

(4) Williams, A. G. B.; Scherer, M. M. Spectroscopic evidence for Fe(II)-Fe(III) electron transfer at the iron oxide-water interface. *Environ. Sci. Technol.* **2004**, *38* (18), 4782–4790.

(5) Pedersen, H. D.; Postma, D.; Jakobsen, R.; Larsen, O. Fast transformation of iron oxyhydroxides by the catalytic action of aqueous Fe(II). *Geochim. Cosmochim. Acta* **2005**, *69* (16), 3967–3977.

(6) Hansel, C. M.; Benner, S. G.; Fendorf, S. Competing Fe(II)-induced mineralization pathways of ferrihydrite. *Environ. Sci. Technol.* **2005**, *39* (18), 7147–7153.

(7) Beard, B. L.; Handler, R. M.; Scherer, M. M.; Wu, L.; Czaja, A. D.; Heimann, A.; Johnson, C. M. Iron isotope fractionation between

aqueous ferrous iron and goethite. *Earth Planet. Sci. Lett.* **2010**, *295* (1−2), 241–250.

(8) Matsuhisa, Y.; Goldsmith, J. R.; Clayton, R. N. Mechanisms of hydrothermal crystallization of quartz at 250 °C and 15 kbar. *Geochim. Cosmochim. Acta* **1978**, *42* (2), 173–182.

(9) Maliva, R. G.; Knoll, A. H.; Simonson, B. M. Secular change in the Precambrian silica cycle: Insights from chert petrology. *Geol. Soc. Am. Bull.* **2005**, *117* (7), 835–845.

(10) Jones, A. M.; Collins, R. N.; Rose, J.; Waite, T. D. The effect of silica and natural organic matter on the Fe(II)-catalysed transformation and reactivity of Fe(III) minerals. *Geochim. Cosmochim. Acta* **2009**, *73* (15), 4409–4422.

(11) Mayer, T. D.; Jarrell, W. M. Formation and stability of iron(II) oxidation products under natural concentrations of dissolved silica. *Water Res.* **1996**, *30* (5), 1208–1214.

(12) Schwertmann, U.; Cornell, R. M., *Iron Oxides in the Laboratory: Preparation and Characterization*; VCH: New York, NY, 1991.

(13) Karim, Z. Characterization of ferrihydrites formed by oxidation of FeCl$_2$ solutions containing different amounts of silica. *Clay Clay Miner.* **1984**, *32* (3), 181–184.

(14) Quin, T. G.; Long, G. J.; Benson, C. G.; Mann, S.; Williams, R. J. P. Influence of silicon and phosphorus on structural and magnetic properties of synthetic goethite and related oxides. *Clay Clay Miner.* **1988**, *36* (2), 165–175.

(15) Carta, D.; Casula, M. F.; Corrias, A.; Falqui, A.; Navarra, G.; Pinna, G. Structural and magnetic characterization of synthetic ferrihydrite nanoparticles. *Mater. Chem. Phys.* **2009**, *113* (1), 349–355.

(16) Drits, V. A.; Sakharov, B. A.; Salyn, A. L.; Manceau, A. Structural model for ferrihydrite. *Clay Miner.* **1993**, *28*, 185–207.

(17) Manceau, A.; Drits, V. A. Local structure of ferrihydrite and feroxyhite by EXAFS spectroscopy. *Clay Miner.* **1993**, *28*, 165–184.

(18) Stookey, L. Ferrozine − a new spectrophotometric reagent for iron. *Anal. Chem.* **1970**, *42*, 779–781.

(19) Clesceri, L.; Greenberg, A.; Eaton, A., *Standard Methods for the Examination of Water and Wastewater*; American Public Health Association, American Water Works Association, and Water Environment Federation, 1989.

(20) Beard, B. L.; Johnson, C. M.; Skulan, J. L.; Nealson, K. H.; Cox, L.; Sun, H. Application of Fe isotopes to tracing the geochemical and biological cycling of Fe. *Chem. Geol.* **2003**, *195* (1−4), 87–117.

(21) Johnson, C. M.; Skulan, J. L.; Beard, B. L.; Sun, H.; Nealson, K. H.; Braterman, P. S. Isotopic fractionation between Fe(III) and Fe(II) in aqueous solutions. *Earth Planet. Sci. Lett.* **2002**, *195* (1−2), 141–153.

(22) Welch, S. A.; Beard, B. L.; Johnson, C. M.; Braterman, P. S. Kinetic and equilibrium Fe isotope fractionation between aqueous Fe(II) and Fe(III). *Geochim. Cosmochim. Acta* **2003**, *67* (22), 4231–4250.

(23) Barrow, N. J.; Bowden, J. W. A comparison of models for describing the adsorption of anions A on a variable charge mineral surface. *J. Colloid Interface Sci.* **1987**, *119* (1), 236–250.

(24) Crosby, H. A.; Roden, E. E.; Johnson, C. M.; Beard, B. L., The mechanisms of iron isotope fractionation produced during dissimilatory Fe(III) reduction by *Shewanella putrefaciens* and *Geobacter sulfurreducens*. *Geobiology* **2007**, DOI: 10.1111/j.1472-4669.2007.00103.x.

(25) Wu, L.; Beard, B. L.; Roden, E. E.; Johnson, C. M. Influence of pH and dissolved Si on Fe isotope fractionation during dissimilatory microbial reduction of hematite. *Geochim. Cosmochim. Acta* **2009**, *73* (19), 5584–5599.

(26) Wu, L.; Beard, B. L.; Roden, E. E.; Kennedy, C. B.; Johnson, C. M. Stable Fe isotope fractionation produced by aqueous Fe(II)-hematite surface interactions. *Geochim. Cosmochim. Acta* **2010**, *74* (15), 4249–4265.

(27) Poulson, R. L.; Johnson, C. M.; Beard, B. L. Iron isotope exchange kinetics at the nanoparticulate ferrihydrite surface. *Am. Mineral.* **2005**, *90*, 758–763.

(28) Schauble, E. A. Applying stable isotope fractionation theory to new systems. *Rev. Mineral. Geochem.* **2004**, *55* (1), 65–111.

(29) Schauble, E. A.; Meheut, M.; Hill, P. S. Combining metal stable isotope fractionation theory with experiments. *Elements* **2009**, *5* (6), 369–374.

(30) Szytuta, A.; Burewicz, A.; Dimitrijevic, Z.; Krasnicki, S.; Rzany, H.; Todorovic, J.; Wanic, A.; Wolski, W. Neutron diffraction studies of a-FeOOH. *Phys. Status Solidi A* **1968**, *26*, 429–434.

(31) Blake, R. L.; Hessevick, R. E.; Zoltai, T.; Finger, L. W. Refinement of hematite structure. *Am. Mineral.* **1966**, *51*, 123–129.

(32) Polyakov, V. B.; Mineev, S. D. The use of Mössbauer spectroscopy in stable isotope geochemistry. *Geochim. Cosmochim. Acta* **2000**, *64* (5), 849–865.

(33) Polyakov, V. B.; Clayton, R. N.; Horita, J.; Mineev, S. D. Equilibrium iron isotope fractionation factors of minerals: Reevaluation from the data of nuclear inelastic resonant X-ray scattering and Mössbauer spectroscopy. *Geochim. Cosmochim. Acta* **2007**, *71* (15), 3833–3846.

(34) Blanchard, M.; Poitrasson, F.; Méheut, M.; Lazzeri, M.; Mauri, F.; Balan, E. Iron isotope fractionation between pyrite (FeS$_2$), hematite (Fe$_2$O$_3$) and siderite (FeCO$_3$): A first-principles density functional theory study. *Geochim. Cosmochim. Acta* **2009**, *73* (21), 6565–6578.

(35) Rustad, J. R.; Casey, W. H.; Yin, Q.-Z.; Bylaska, E. J.; Felmy, A. R.; Bogatko, S. A.; Jackson, V. E.; Dixon, D. A. Isotopic fractionation of Mg^{2+}(aq), Ca^{2+}(aq), and Fe^{2+}(aq) with carbonate minerals. *Geochim. Cosmochim. Acta* **2010**, *74* (22), 6301–6323.

(36) Dzombak, D. A.; Morel, F. M. M., *Surface Complexation Modeling: Hydrous Ferric Oxide*; John Wiley & Sons: New York, 1990.

(37) Johnson, C. M.; Beard, B. L.; Klein, C.; Beukes, N. J.; Roden, E. E. Iron isotopes constrain biologic and abiologic processes in banded iron formation genesis. *Geochim. Cosmochim. Acta* **2008**, *72* (1), 151–169.

(38) Rouxel, O.; Sholkovitz, E.; Charette, M.; Edwards, K. J. Iron isotope fractionation in subterranean estuaries. *Geochim. Cosmochim. Acta* **2008**, *72* (14), 3413–3430.

(39) Hill, P. S.; Schauble, E. A.; Shahar, A.; Tonui, E.; Young, E. D. Experimental studies of equilibrium iron isotope fractionation in ferric aquo-chloro complexes. *Geochim. Cosmochim. Acta* **2009**, *73* (8), 2366–2381.

(40) Kappler, A.; Johnson, C. M.; Crosby, H. A.; Beard, B. L.; Newman, D. K. Evidence for equilibrium iron isotope fractionation by nitrate-reducing iron(II)-oxidizing bacteria. *Geochim. Cosmochim. Acta* **2010**, *74* (10), 2826–2842.

(41) Skulan, J. L.; Beard, B. L.; Johnson, C. M. Kinetic and equilibrium Fe isotope fractionation between aqueous Fe(III) and hematite. *Geochim. Cosmochim. Acta* **2002**, *66* (17), 2995–3015.

(42) Tangalos, G. E.; Beard, B. L.; Johnson, C. M.; Alpers, C. N.; Shelobolina, E. S.; Xu, H.; Konishi, H.; Roden, E. E., Microbial production of isotopically light iron(II) in a modern chemically precipitated sediment and implications for isotopic variations in ancient rocks. *Geobiology* **2010**, *8* (3), 197−208.

F

dx.doi.org/10.1021/es103171x |*Environ. Sci. Technol.* XXXX, XXX, 000–000